International Journal of Rotating Machinery, 10: 1–13, 2004

ISSN: 1023-621X print
DOI: 10.1080/10236210490258016

Taylor & Francis
Taylor & Francis Group

Pumping Speed Measurement and Analysis for the Turbo Booster Pump

R. Y. Jou, S. C. Tzeng, and J. H. Liou
Department of Mechanical Engineering, Chien Kuo Institute of Technology, Changhua, Taiwan, Republic of China

This study applies testing apparatus and a computational approach to examine a newly designed spiral-grooved turbo booster pump (TBP), which has both volume type and momentum transfer type vacuum pump functions, and is capable of operating at optimum discharge under pressures from approximately 1000 Pa to a high vacuum. Transitional flow pumping speed is increased by a well-designed connecting element. Pumping performance is predicted and examined via two computational approaches, namely the computational fluid dynamics (CFD) method and the direct simulation Monte Carlo (DSMC) method. In CFD analysis, comparisons of measured and calculated inlet pressure in the slip and continuum flow demonstrate the accuracy of the calculation. Meanwhile, in transition flow, the continuum model of CFD is unsuitable for calculating such rarefied gas. The pumping characteristics for a full 3D model on a rotating frame in transition and molecular regimes thus are simulated using the DSMC method and then confirmed experimentally. However, when the Knudsen number is in the range $0.5 < Kn < 0.1$, neither CFD computation nor DSMC simulation is suitable for analyzing the pumping speed of the turbo booster pump. In this situation, the experimental approach is the most appropriate and effective method for analyzing pumping speed. Moreover, the developed pump is tested using assessment systems constructed according to ISO and JVIS-005 standards, respectively. Comparisons are also made with other turbo pumps. The compared results show that the turbo booster pump presented here has good foreline performance.

Keywords CFD, DSMC, Flow meter method, Transition flow, Turbo booster pump

Received 19 June 2002; accepted 31 December 2002.
The National Science Council under the contract number of NSC90-2212-P-270-001 provides supports for this work. All authors deeply appreciate the experimental support of Precision Instrument Development Center, National Science Council in Taiwan. Support of Ms. Y. W. Chang in DSMC simulation and Dr. H. P. Cheng in CFD calculation is also highly appreciated. Both of them have done much excellent research in this field.
Address correspondence to R. Y. Jou, Department of Mechanical Engineering, Chien Kuo Institute of Technology, Changhua 500, Taiwan, Republic of China. E-mail: ryjou@ckit.edu.tw

INTRODUCTION

Review of the Turbo Pump Designs

Plasma-based etch and chemical vapor deposition (CVD) depend on the reaction of gas molecules and reactive ions on the wafer surface. The concentration, arrival rate and directionality of reactive gases and ions determine the etching rate, deposition rate, step coverage, process uniformity, and etching profile. Meanwhile, the parameters of concentration, arrival rate and directionality are in turn determined by flow rates and chamber pressure, as well as by plasma energy and the distance between the plasma and wafer. The above two processes differ from alternatives in that they require high flow rates, and relatively shallow vacuum levels. Specifically, pressures of around 10 mTorr are required, along with flow rates of up to 800 SCCM. Those requirements become increasingly stringent with the move to 300 mm wafer and 0.25 to 0.18 μm designs. Consequently, pumps used for pumping CVD or etching equipment in the IC industry require superior discharge characteristics in conditions ranging from atmospheric pressure to a high vacuum.

Momentum transfer from the high-speed rotating blades to the gas molecules affects the action of a turbomolecular pump (TMP). In molecular drag pump (MDP) designs, the pumped fluid generally moves parallel to the moving wall, while in TMP designs the movement is perpendicular. Maurice (1974) proposed a significant improvement to the MDP design that enhanced pump compression ability by reducing the influence of internal leakage. Moreover, Henning (1988) reviewed 30 years of turbo type and turbodrag type pump design to trace the development of turbo pumps. Furthermore, Duval et al. (1988) discussed the development history of molecular pumps. Duval et al.

noted that modern MDP possess some interesting characteristics, particularly a high compression ratio in the viscous flow range, enabling MDP to operate as a booster and to operate in the 10^{-2} to 10^{-1} mbar at full pumping speed. Sawada et al. (1990, 1992, 1993) proposed an analytical method for investigating the pumping performance of spiral grooved visco-vacuum pumps with arbitrary groove cross-sections. Moreover, Sawada et al. also experimentally assessed this theoretical model.

Cleanliness is an important consideration in vacuum turbo pump design. The most common method of ensuring cleanliness involves increasing the tolerable discharge pressure to allow the use of oil-free backing pumps. The compound turbo pump, which complements the conventional TMP design by incorporating a turbo-drag section on the same rotation shaft, permits discharge pressures of 1000 to 2000 Pa. Meanwhile, Levi (1992) developed another type of pump, called a hybrid pump, which combines different impellers on the same axis without increasing the number of stages. Furthermore, Hablanian (1994) reviewed the development history of turbine-type, high vacuum pumps and noted that the optimization process for designing a general-purpose turbopump for high-vacuum use is incomplete. Finally, Heldner and Kabelitz (1990) compared the design and performance characteristics of the most widely used rolling element bearing system to more advanced bearing systems and noted that fully magnetic bearing designs are growing in popularity, and becoming a design standard for IC industry application. Table 1 briefly lists some basic characteristics of the TMP, MDP, and compound molecular pump (CMP).

The main advantage of compound turbo pumps is that they can exhaust at relatively high pressures, so high that simple, dry diaphragm pumps can be used for backing. Turbo pumps also are often used as an upstream booster or "supercharger" for a Roots blower, which has poor throughput in low milliTorr pressure ranges, but pumping speed still tends to decline. Currently, various pumps combining the traditional design principles of Gaede (1913), Holweck (1923), Siegbahn (1943), and Becker (1961) are being proposed. These designs generally improve pumping performance in certain ways, including either pumping speed or compression ratio. Because of uncertainty regarding natural and treatment difficulties of the transitional flow problem, it is difficult or even impossible to improve pumping speed and compression ratio simultaneously, especially at higher exhaust pressure. Jou et al. (2000) presented a turbo booster pump (TBP) with smooth and good performance in the transition regime. As shown in Figure 1, this design has a compact structure compared with other available designs and differs significantly from available methodologies in terms of design principles.

Analysis and Simulation for Turbo Pump Designs

Regarding the numerical analysis of turbo vacuum pumps, Lee and Lee (1996) investigated the compression characteristics for a simplified drag pump model. Moreover, Schneider et al. (1998) built an empirical and 2D numerical calculation for a single stage turbomolecular pump. Additionally, Nanbu et al. (1991) applied DSMC to design spiral grooves on a turbomolecular pump rotor. Heo and Hwang (2000) also used DSMC to calculate the blade row of a TMP in the molecular and transition flow regions. Heo and Hwang concluded that the maximum compression ratio and pumping speed depend strongly on the Knudsen number in the transition region, and also depend weakly on the Knudsen number in the free molecular flow region. In those studies, when dealing with the simulation of turbomolecular pumps, it is usual to fix the analysis model on the rotating rotor and make some assumptions and simplifications. Owing to the geometrical characteristics of the turbo booster pump rotor, as depicted in Figure 2, Chang et al. (2001) proposed a full 3D DSMC model on a rotating frame that included the design parameters of clearance between the rotor and the stator and blade thickness. Additional treatments related to Coriolis acceleration

TABLE 1
Characteristic List of TMP, MDP, and CMP

	TMP	MDP	CMP (TMP + MDP)
Rotor configuration	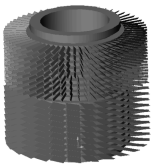	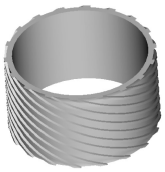	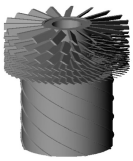
Pumping speed	High	Relatively small	High
Foreline pressure	Very low (<1 Pa)	High (1000 to 2000 Pa)	High (1000 to 2000 Pa)
Transitional flow performance	Poor	Good	Good
Structure	Complex	Compact	Complex; with TMP element Compact; without TMP element
Manufacture	Difficult	Easy	Difficult; with TMP element Easy; without TMP element

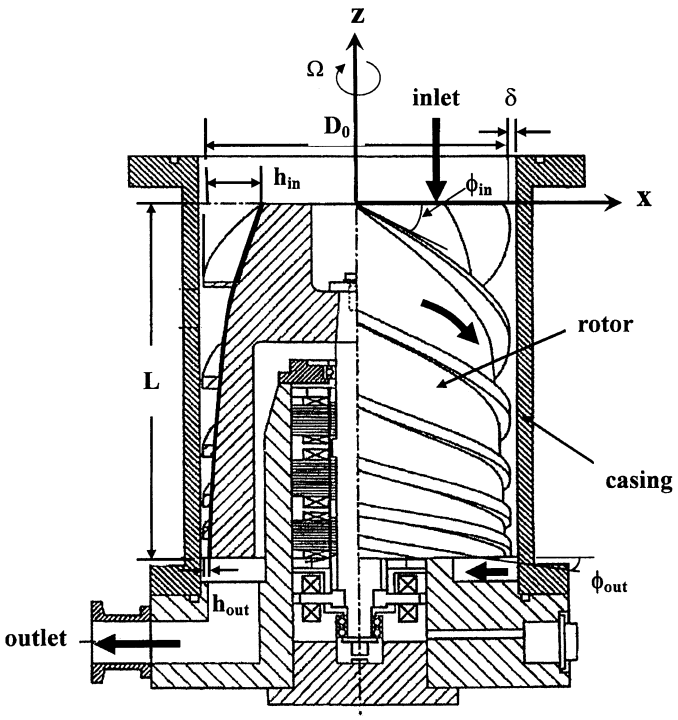

D=206.8mm L=240mm δ=0.5mm
h_{in}=58.4mm h_{out}=4mm
ϕ_{in}=30° ϕ_{out}=12.5°

FIGURE 1
Schematic drawing of the spiral-grooved turbo booster pump with a five DOF actively controlled magnetic bearing (AMB) system.

and centripetal acceleration are done using the DSMC method. Finally, Cheng et al. (2000) used CFD calculation to examine the flow field of this turbo booster pump. Comparisons of measured and calculated inlet pressure in the slip and continuum flow demonstrated that the calculation was quite accurate. However, the continuum model of CFD in unsuitable in terms of transition flow for calculating such rarefied gas.

PERFORMANCE TESTING APPARATUS

Numerous standards exist for evaluating turbomolecular pump performance, including ISO/CD5302, AVS 4.1, 4.2, 4.3, DIN28428, JVIS-005 and so on. However, these testing specifications contain some discrepancies. One issue is especially important in turbo pump testing. Since the operating pressure range of turbomolecular pumps differs from that of compound or hybrid turbo pumps, the elongated operating foreline pressure of composite-type pumps requires detailed consideration. The present standard is only applicable to turbomolecular pump testing, and is unable to assess functions of compound turbo pumps. However, to provide preliminary testing results for research, this study adopts the original standard specifications for turbomolecular pump testing.

To test the entire operating range of the turbo pumps, a system that combines the measurement functions of the flow meter and orifice methods should be developed. This approach would facilitate the calculation of pumping speeds under a constant inlet pressure condition based on the stable chamber pressure, mass flow into the chamber, conductance of the orifice, and the final base pressure of the system. The equation for evaluating pumping speeds adopted in ISO/CD5302 is presented below.

Flow Meter Method

The steady pressure method is adopted to measure the volume flow rate S by the determined gas throughput Q. Given constant pressure P_1 in a given area of the test dome (Figure 3a), which is measured by a pressure gauge, the volume flow rate S is obtained by the relationship

$$S = \frac{Q}{P_1 - P_0} \qquad [1]$$

where P_0 denotes the ultimate operational pressure in the test dome.

Orifice Method

The method adopted to measure the volume flow rate S is the steady pressure "standard conductance" method in which a thin orifice plate divides the test dome (Figure 3b) into two volumes. If the pressure in each volume is measured by pressure gauges with the same sensitivity, the volume flow rate is given by

$$S = C\frac{P_1}{P_2 - 1} \qquad [2]$$

where C denotes the calculated conductance taking account of the orifice size and gas properties. The orifice conductance is evaluated by following equation

$$C = \frac{\pi RT}{32M}\frac{1}{(1 + L_o/d)}d^2 \qquad [3]$$

where L denotes the thickness of the orifice plate, the universal gas constant R equals 8314 N-m/(mol-K), and the molecule weight of air is 28.8×10^{-3} Kg/mol. Finally, the term $1/(1 + L_o/d)$ represents a correction-factor which can be defined as the average throughput probability.

Jou et al. (2000) designed a testing system for investigating the performance of the turbo booster pump under high inlet pressure. The system complies with ISO standards, and can be applied to pumping speed testing using the flow meter method. Figure 4 displays the schematic layout of this system. The system includes a testing chamber, auxiliary pumping system, vacuum gauges, mass flow meters, and an RGA. Table 2 presents

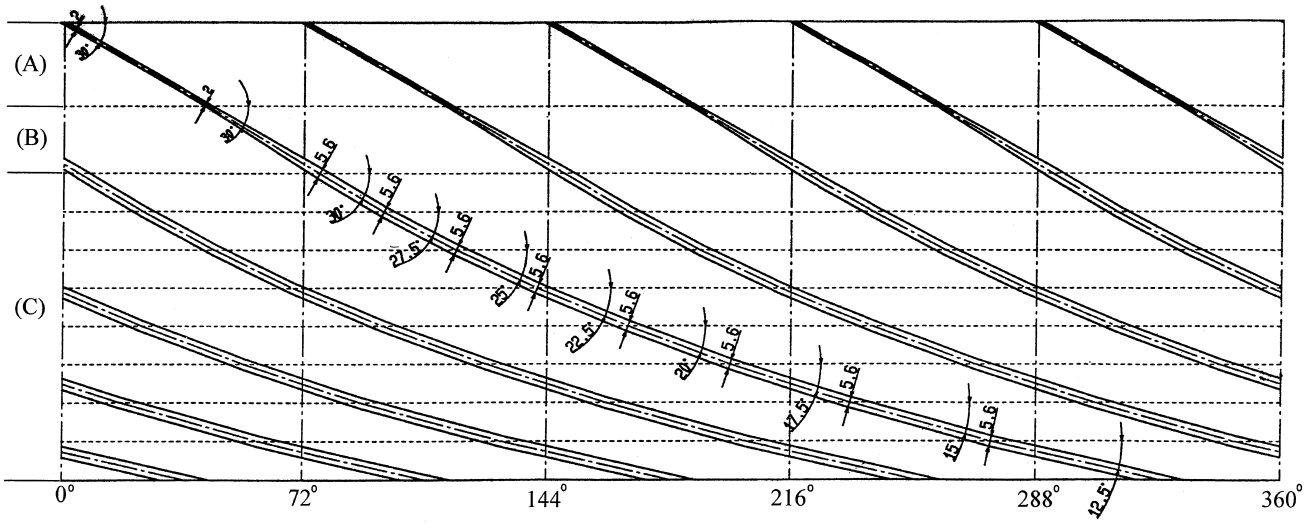

(A) TMP section: Z = 0 ~ 45mm, D_0 = 90 ~ 139.4mm
(B) connecting element: Z = 45 ~ 80mm, D_0 = 139.4 ~176.8mm
(C) spiral-grooved helix: Z =80 ~ 240mm, D_0 = 176.8 ~ 198.8mm

(a)

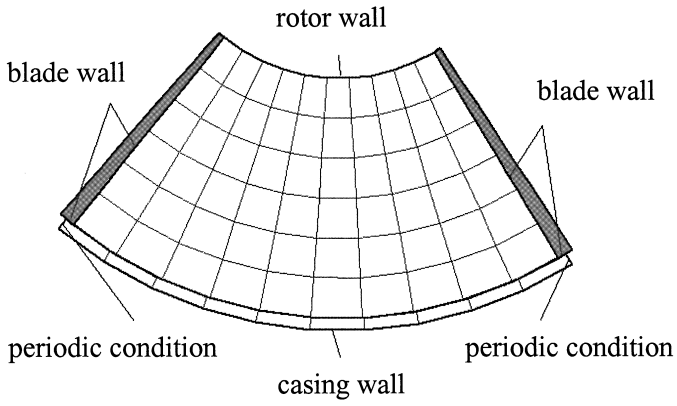

(b)

FIGURE 2

(a) Rotor configuration of the spiral-grooved turbo booster pump. (b) Computational domain and boundary conditions for each surface of the turbo booster pump's rotor.

the major testing functions of the system. A testing apparatus constructed by Kashiyama Co. Ltd. in Japan is adopted to compare the testing functions of the ISO and JVIS standards. Table 3 briefly compares these two testing systems. In these apparatus, a series of precision flow meters with different measurement range are installed to adjust the rate of nitrogen flow into the chamber. Furthermore, pressure gauges of a B-A gauge for ultimate pressure indication in high vacuum measurements, and a set of Baratron gauges for low vacuum measurements are attached to the system to measure the equilibrium pressure inside the testing chamber. Pumping performance can easily be assessed by flow meter and pressure gauge readings.

PUMPING ANALYSIS BY CFD AND DSMC METHODOLOGIES

Numerical simulation of vacuum pump flow provides detailed information on fluid flow field during flow through the pumping channels. Important benefits of the numerical approach include sufficient accuracy for engineering designs, fast response to design changes (for example through eliminating a lengthy trial-and-error process), and saving on prototype development costs since the design performance can be simulated and displayed on a computer before actual pump manufacture. Depending on operating pressure ranges, two approaches are commonly used to examine and characterize a pumping flow in detail. Specifically, the computational fluid dynamics (CFD)

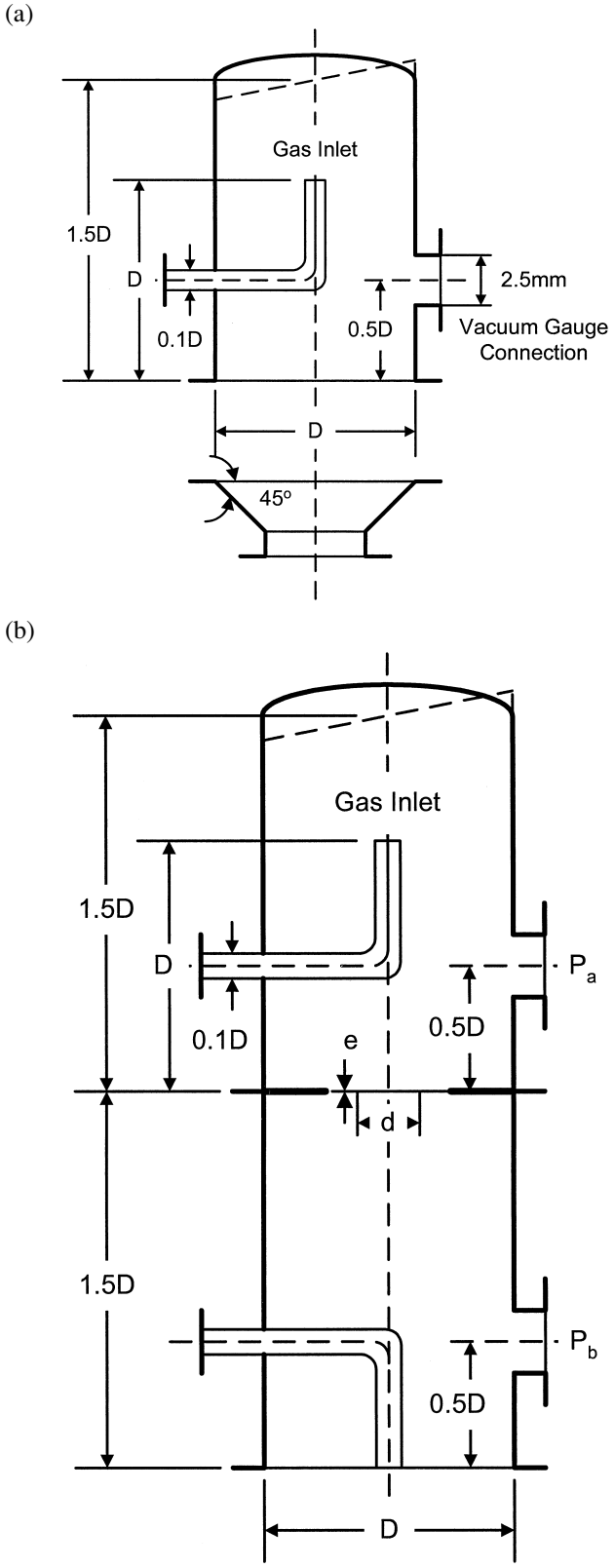

FIGURE 3
Test domes of ISO/CD5302. (a) Flow meter method, (b) orifice method.

methodology is used to analyze continuum flows and the direct simulation Monte Carlo (DSMC) method is used for the molecular flow simulation.

The Knudsen number, Kn in Table 4, which is defined as a ratio of mean free path to a characteristic rotor length (such as the groove depth), is used to distinguish the flow regimes and identify the most appropriate method for adoption. No clear difference exists between the suitability of the CFD and DSMC methods, both of which suffer limitations in transitional flow regimes (in the approximate range $0.1 < \mathrm{Kn} < 10$). Consequently, computations should be conducted to cover this range as large as possible. Figure 5 outlines the entire procedure in flowchart form. According to the design requirements, analyses are conducted sequentially from low to high vacuum levels.

When inlet pressure follows a viscous flow regime (normally $\mathrm{Kn} < 0.1$, but calculations are performed for the upper limit of Kn), based on a set of prescribed inlet conditions and outlet mass flow conditions, the CFD approach is used to calculate the inlet pressures achieved by the pump. The turbo booster pump analysis makes the following basic assumptions.

1. Flow field is a laminar.
2. Gases satisfy the Newtonian constitutive law.
3. Gases are ideal and satisfy the state equation for an ideal gas.
4. Flow is isothermal.

The CFD code, UNIC, employs finite difference approximations to discretize transport equations on body-fitted grid-mesh systems. Specifically, the simulation uses an adoptive third-order upwind total variation diminishing (TVD) scheme to approximate the convective parts of the transport equations. Moreover, the simulation uses a second-order central differencing scheme for the viscous and source terms of the governing equations. The present simulation also uses a pressure-based predicted/corrector solution procedure to enhance the velocity-pressure coupling and mass-conserved flow field solutions at the end of each time step. Finally, an implicit Euler time-marching scheme is used to enhance the convergence for steady-state flows. The coordinates used for the analyses are fixed on the rotor, which rotates at a constant speed. From the calculation, the gas pressure distribution along the pumping channel, pressure difference between pump inlet and outlet, and gas pumping flow rate can be predicted with reasonable accuracy. For compressible flow computations such as vacuum pumping, a state equation of the following form is employed to close the governing equations.

$$\rho = \frac{P}{\left(\frac{R}{M}T\right)} \qquad [4]$$

As illustrated in Figure 2b, the boundary conditions for the vacuum pumping flow analysis considered here include setting the inlet condition to a fixed volume flow rate, and an absence of slip motion of molecules on the wall. A periodic boundary condition is subjected for each periodic computational domain.

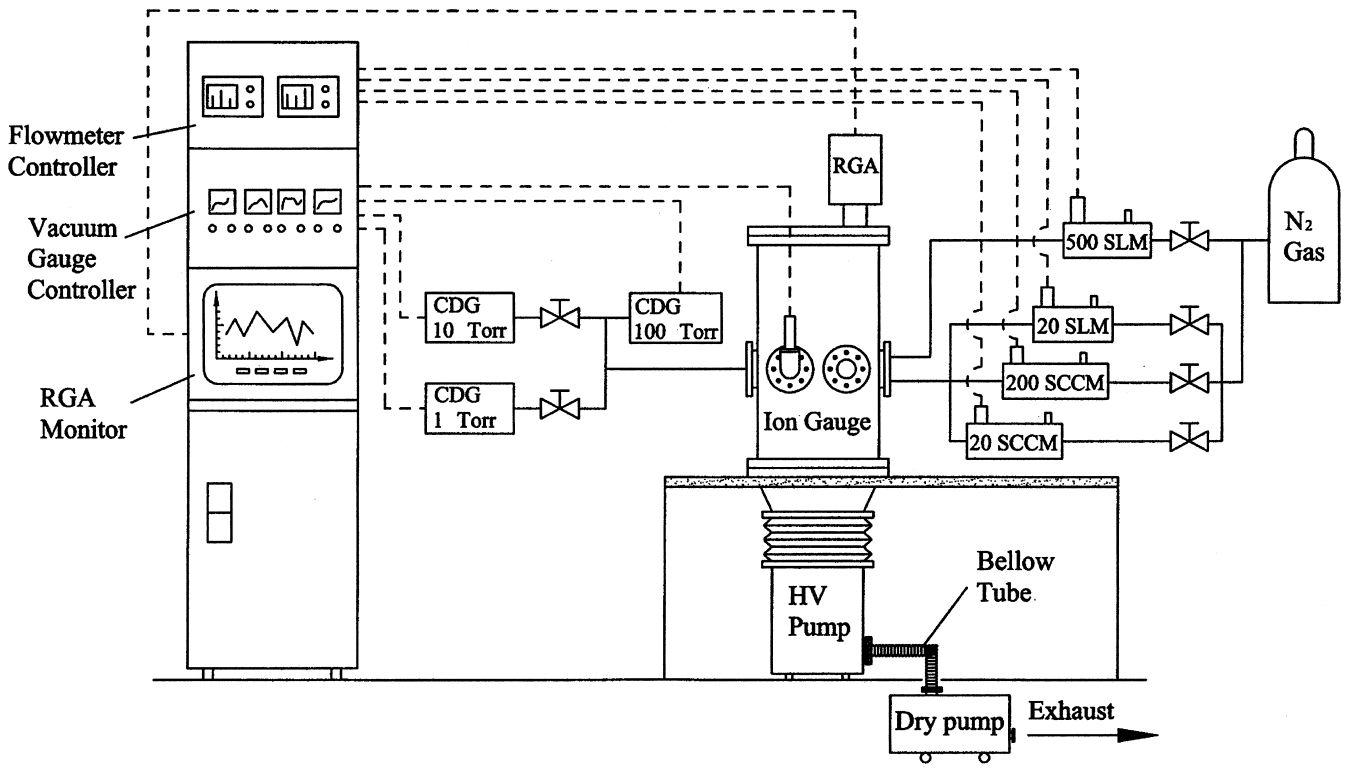

FIGURE 4
Schematic layout of the measurement system designed by the flow meter method following the ISO testing specification.

DSMC simulation is utilized to calculate the pumping characteristics of the turbo booster pump when its operating inlet pressure is in the molecular flow regime (normally Kn $>$ 10, but calculations must be extended to the lower limit of Kn). The DSMC methodology involves the computerized simulation of molecular kinetics. The transport terms in the Navier-Stokes equations of the continuum gas dynamics fail when the gradients of the macroscopic variables become so steep that their scale length is of the same order as the average distance traveled by the molecules between collisions, or the mean free path. Essentially, except for the solver, the computational procedure of DSMC scheme is similar to that of the CFD scheme, as shown in Figure 5.

In DSMC analysis, for the sake of consistency, the following values are fixed; (a) throughput, which can be expressed as $Q = P_{\text{in}} S_{\text{in}} = P_{\text{out}} S_{\text{out}}$ (where P denotes pressure, S represents pumping speed, and subscripts in and out denote inlet and outlet respectively), and (b) pressure at the outlet, namely P_{out}. Given equal flow outside the inlet and outlet ports, the outlet influx can be easily determined based on kinetic theory, yet the inlet influx $N'_{\text{in},i}$ cannot be determined because of the unknown P_{in} and S_{in}. Consequently, the following iterative procedures for adjusting

TABLE 2
Functions of the Turbo Pump Testing System

Items	Instruments	Testing ranges
Ultimate pressure	GP360 Ionization gauge	$7\times10^{-4}\sim7.5\times10^{-10}$ Torr
Pumping speed	MKS Baratron 690 Capacitance diaphragm gauge	1 atm$\sim10^{-4}$ Torr
Throughput	Kofloc 3920 Sierra Sidetrak 840 Mass flow meter	$<$1SCCM, 0$\sim$20 SCCM 0$\sim$200 SCCM, 0$\sim$2 SLM 0$\sim$20 SLM, 0$\sim$500 SLM
Residual gas	Blazers QME-200 Residual gas analyzer	0$\sim$300 amu

TABLE 3
Comparisons of Testing Systems Designed by ISO and JVIS Standards

PIDC system (ISO)	Kashiyama system (JVIS)
Ion gauge (GP 360)	B-A gauge (for ultimate pressure)
CDG (1 Torr, 10 Torr, 1000 Torr)	Schultz gauge
	CDG
1SCCM, 20SCCM, 200SCCM, 2SLM, 20SLM	30SCCM, 100SCCM, 500SCCM, 2SLM, 10SLM, 50SLM

the given conditions are used to provide the given throughput Q and outlet pressure P_{out}. (1) First, P_{in} is assigned an initial value based on an estimate, then the inlet influx is determined by applying the continuity condition of mass at the boundary. (2) Next, one time step of the DSMC calculation is performed, and the number of the incoming and outgoing molecules (denote as $N_{\text{in},i}$ and $N_{\text{in},o}$ respectively) at the inlet entrance during the time step are recorded. (3) Finally, the inlet pressure of the next time step is calculated using the following relationships. The inlet influx then can be determined.

$$U_{\text{in}} = \frac{N_{\text{in},i} - N_{\text{in},o}}{A_{\text{in}} n_{\text{in}} \Delta t} \quad [5]$$

$$S_{\text{in}} = U_{\text{in}} A_{\text{in}} \quad [6]$$

$$P_{\text{in}} = \frac{Q}{S_{\text{in}}} \quad [7]$$

In the above equations, A_{in} denotes the inlet area, and U_{in} represents the free stream velocity outside the inlet port.

Steps (2) and (3) are repeated until the inlet pressure stabilizes. Several methods of improving the convergence exist. In this work steps (2) and (3) are not performed until the initial flow is well developed and the incoming and outgoing molecules are substituted by time average values in Equation (5). Because of the limited number of simulated molecules, the resulting P_{in} of each step fluctuates slightly even when the steady state has been reached. This fluctuation is statistical is nature, and should decrease with increasing number of incoming and outgoing simulated molecules at each step. Consequently, the criterion for the attainment of a steady value for P_{in} used in this investigation is that the relative difference between the average value of P_{in} in the previous two thousand steps and the following two thousand steps is below 0.5%.

RESULTS AND DISCUSSION

The rotor configuration presented in Figure 2 is the design examined in this study. This rotor is operated at 24000 rpm. The rotor diameter is 206 mm and the axial rotor length is 240 mm. Moreover, the rotor contains five blades. This design includes a group of spiral blades embedded in a cylinder, a pump casing, and a single cylindrical rotor coaxially arranged within the pump casing. Each blade comprises three different elements that are continuously linked. The blade characteristics comprise a dynamic-vane element on the inlet side, a spiral-grooved element on the exhaust side, and a connecting element linked the dynamic-vane and the spiral-grooved element continuously together. TMP design philosophy is a basis for dynamic-vane design, and viscous flow theory forms the basis of the spiral-groove design. Each blade characteristic, such as section angle, blade thickness, axial length, and so on, is carefully designed to satisfy the operating principles of molecular flow pumping, viscous flow pumping, and smooth transition flow pumping. The design aims to optimize performance when gases are pumped along the axial direction. Thus, even when gas flow is disturbed by sudden blade shape variation inside the pumping channel, discharge efficiency is not compromised.

To identify the discrepancies between the ISO and JVIS testing standards, the turbo booster pump backed by a 1500 l/min foreline pump (SD90VIII) is tested in each system, respectively. As illustrated in Figure 6, the pumping speeds vary by 40% in for inlet pressure of 0.01 Pa to 1 Pa. Moreover, when the inlet pressure exceeds 1 Pa, the deviation between these two testing results is below 10%. When inlet pressure is below 10^{-2} Pa, since a GP360 ion gauge is installed on the ISO testing apparatus, the measurement range in the pumping speed can reach the 10^{-3} Pa range. Moreover, when the inlet pressure condition is below the 10^{-3} Pa range, an orifice method other than the flow meter method used here should be adopted to measure the inlet condition up to the ultimate pressure regime.

TABLE 4
Classification of Pumping Flow Regimes

Flow	Knudsen number Kn	Model
Viscous flow	$\text{Kn} < 0.01$	Navier-Stokes eqns. (No-slip BC)
Slip flow	$0.01 < \text{Kn} < 0.1$	Navier-Stokes eqns. (Slip BC)
Transitional flow	$0.1 < \text{Kn} < 10$	Boltzmann eqn.
Free molecular flow	$10 < \text{Kn}$	Collisionless Boltzmann eqn.

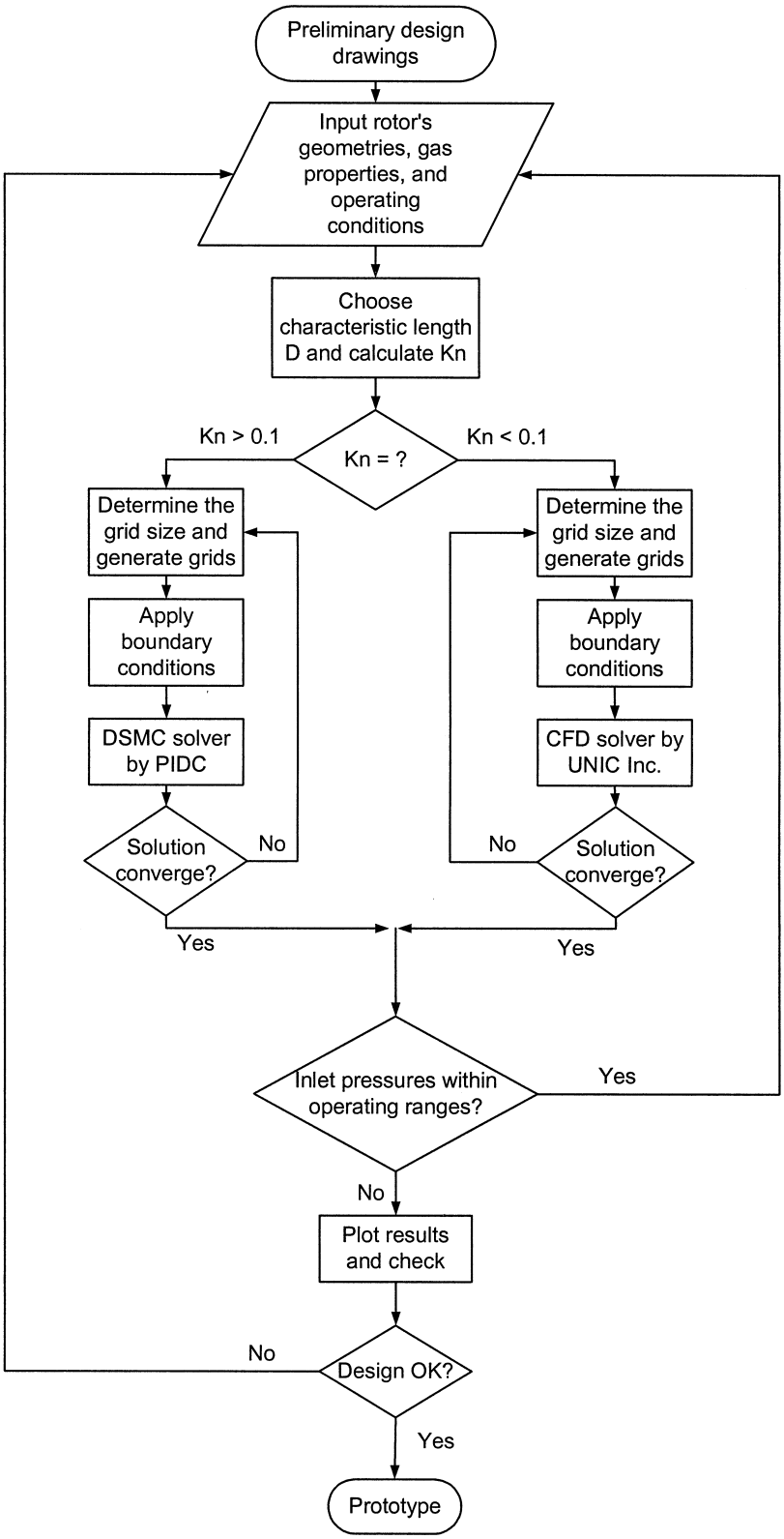

FIGURE 5
Design and simulation procedures for the turbo booster pump development by using CFD and DSMC methodologies.

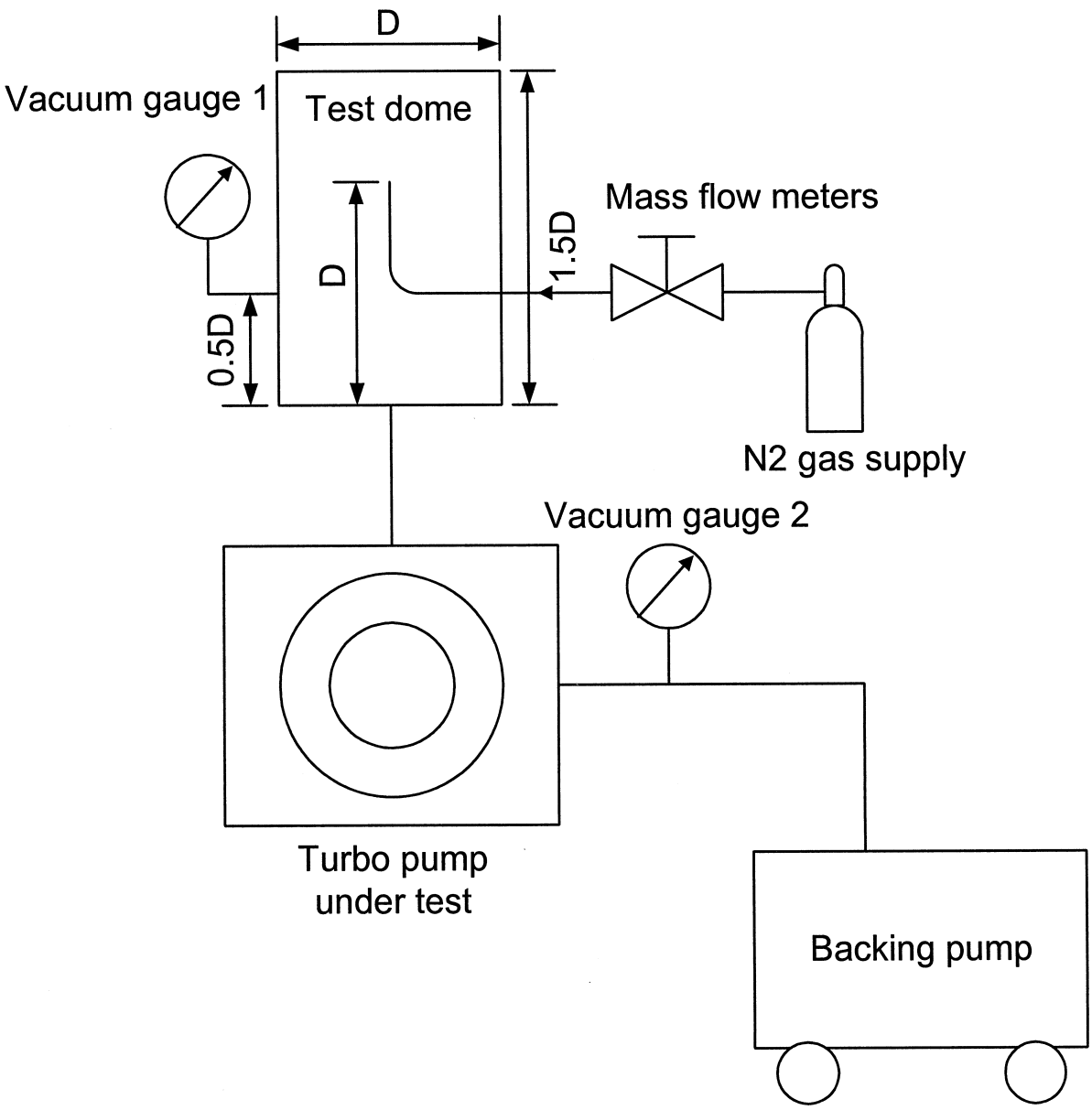

FIGURE 6
Schematic of the pumping speed testing by the flow meter method.

The pumping speed test involves testing the turbo booster pump backed by different foreline pumps or combinations of backing pump and foreline pump. Notably, Figure 6 displays the schematic layout of the testing using the flow meter method. Moreover, Figure 7 plots the pumping speed curves tested using SD90VIII and SD120H as the foreline pumps. The pumping speed specification of SD90VIII is 1500 l/min, while of SD120H is 2000 l/min. As revealed in Figure 7, when inlet pressure exceeds 1 Pa, the testing data of these two system connections varies with pumping speed. This phenomenon reveals the effect of foreline pump size. Below this pressure a plateau region exists for pumping speed, which is independent of the foreline pump used. The maximum pumping speed of this turbo booster pump occurs at the 1000 l/s level. From the test results, the exhaust pressure can reach as high as 1000 Pa. This high exhaust pressure characteristic is very important because it allows the use of a mechanical booster pump to be omitted, thus enabling cheaper, more compact and more reliable systems.

To demonstrate the improvement of pumping performance in the transitional flow of the designed turbo booster pump, a commercialized compound-type turbo pump (Osaka TG1133M with magnetically levitated bearing, as shown in Table 1) is tested in the ISO system. Figure 7 displays the test results. This design combines six stages of TMP blades in the inlet side with

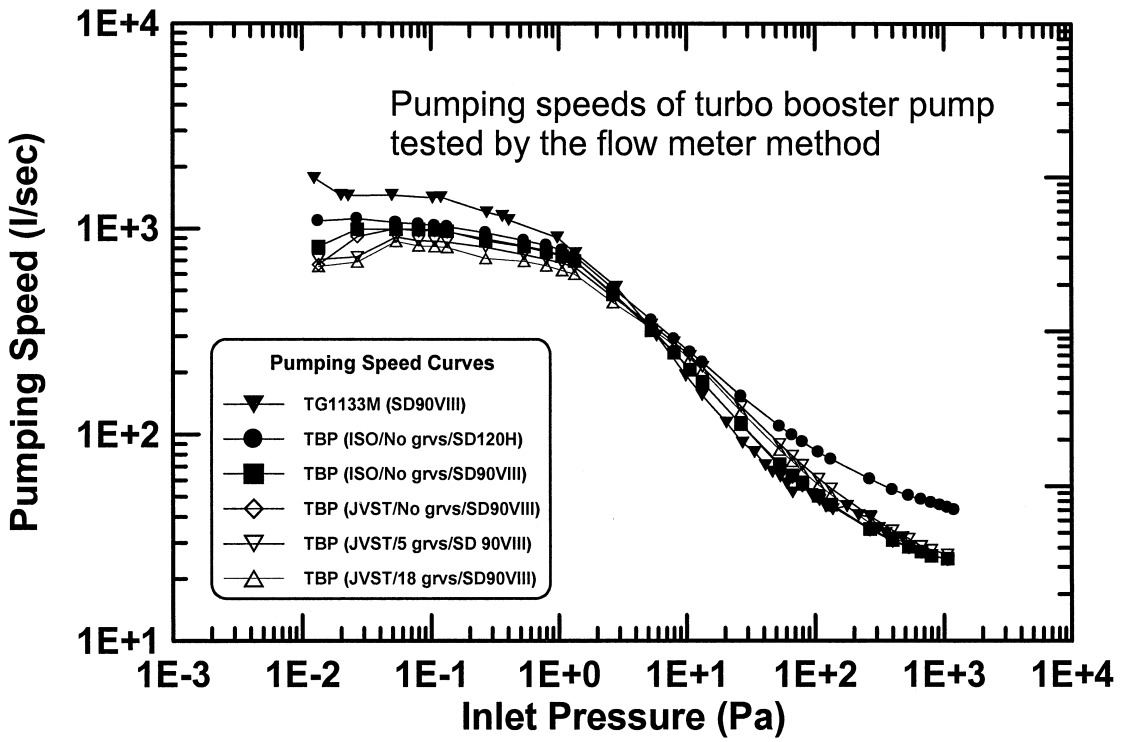

FIGURE 7
Pumping speeds testing of the turbo booster pump backed by a single SD90VIII or SD120H foreline pump.

an eight groove MDP section in the outlet side to enhance its compression ability under a viscous flow regime. The measured ultimate pressure is around 10^{-7} Pa. When inlet pressure exceeds 32 Pa, the compression capability of the MDP section is lower than the turbo booster pump, and its foreline pressure is only 500 Pa, below the 1300 Pa of the turbo booster pump. This compound-type turbo pump requires a more powerful foreline pump to back its pumping. Furthermore, when the inlet pressure is below 5 Pa, since the flow regime is a free molecular flow regime, the traditional TMP mechanism (see Table 1) with multiple interlaced stages of rotor and stator is the most effective design for vacuum pumping. The proposed turbo booster pump has a TMP element (which functions as a rotor) on its inlet side, but lacks a stator, meaning that the pumping speed in this flow regime is less than that of the pump it is compared with. On the other hand, if inlet pressure exceeds 5 Pa, continuum viscous flow dominates the vacuum pumping. A spiral-grooved rotor can maintain the pressure difference between inlet and exhaust. The turbo booster pump design presented in this study has a much larger cross section than the compared pump, as well as a faster pumping speed. Table 5 compares the performance of the turbo booster pump, pump A (Osaka TG1133M), and

TABLE 5
Performance Comparisons of Turbo Vacuum Pumps with Different Rotor Designs

Items	Turbo booster pump	Pump A	Pump B
Size (mm)	ϕ285 × 400	ϕ300 × 360	ϕ253 × 319
Inlet flange (mm)	NW200	DN200CF	ICF253
Rotation speed (rpm)	24000	33600	35000
Pumping speed (67 Pa)	80 l/s	50 l/s	22 l/s
(1.33 Pa)	645 l/s	850 l/s	500 l/s
(0.133 Pa)	860 l/s	1500 l/s	1000 l/s
Max. foreline pressure (Pa)	1300	500	266Pa
Vibration (μm)	<0.01	<0.01	<0.01
Cooling water	1∼4 L/min	Air	Air/Water
Foreline pump	SD90VIII	SD90VIII	?
Note	(Tested by PIDC's system)	(Tested by PIDC's system)	(Data extracted from product's catalog)

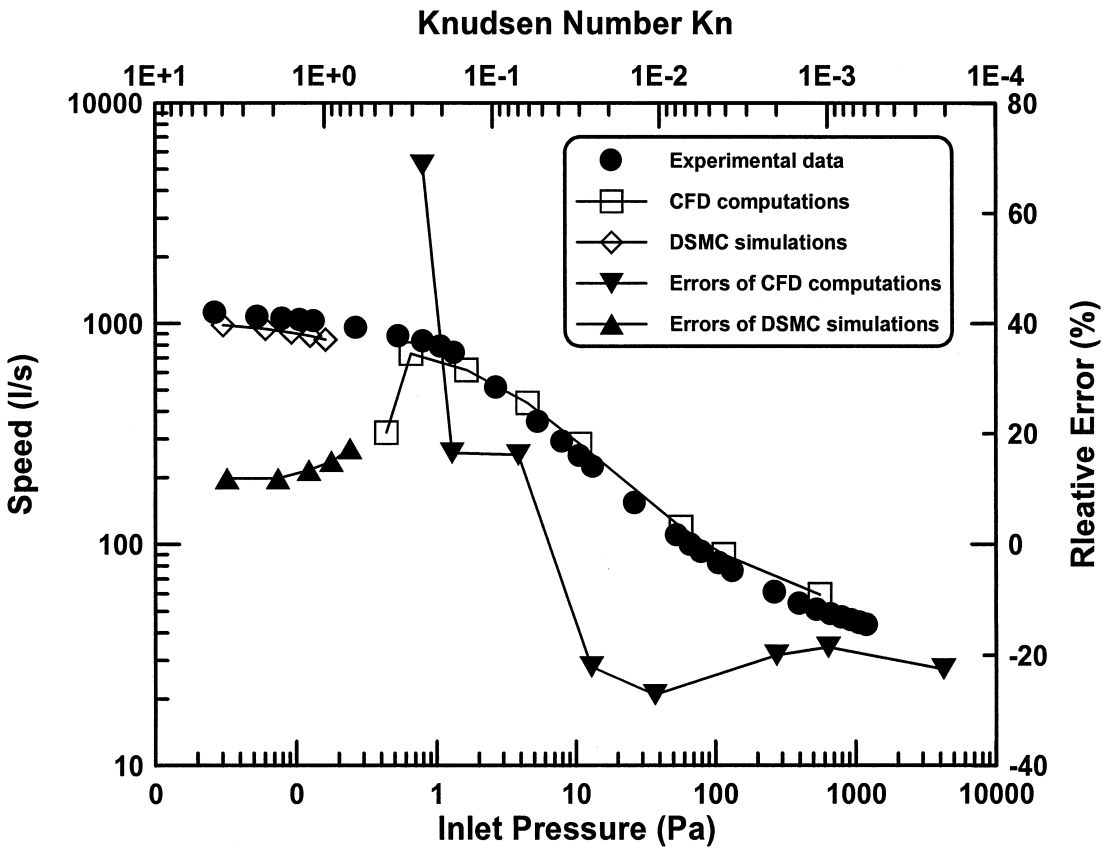

FIGURE 8
Comparisons of experimental measurements and calculations by the CFD and the DSMC methodologies for pumping speeds of the turbo booster pump backed by the SD120H foreline pump.

pump B (Seiko STP-H1000C). The comparison indicates that the pumping speed of the turbo booster pump is best in the transition flow regime.

Figure 8 compares the experimental data with the analysis results of CFD and DSMC methodologies to verify the accuracy of the analysis Meanwhile, Table 6 lists the relevant comparison data. All analyses are conducted using a commercialized CFD package (UNIC) and a self-developed DSMC code based upon Bird's (1994) method. Moreover, calculations are based on the SD120H foreline pump specifications. In the CFD study, the

TABLE 6
Listing of Computational Results and Experimental Data for Pumping Speeds of a Turbo Booster Pump

Scheme	Inlet pressure (Pa) (Computed)	Outlet pressure (Pa) (Fixed conditions)	Computed results (l/sec)	Experimental data (l/sec)	Relative error %
DSMC	0.03	1.87	982.2	1114.8	11.89
	0.06	3.60	943.26	1070.6	11.89
	0.09	5.07	908.31	1049.1	13.42
	0.13	6.27	878.38	1033.2	14.98
	0.16	7.46	843.8	1021	17.36
CFD	0.65	19.06	729.01	873.5	16.54
	1.63	33.33	615.27	734.1	16.19
	4.47	55.85	435.66	356.9	-22.07
	10.73	80.38	283.52	223	-27.14
	56.87	164.49	119.03	99.2	-19.99
	115.16	244.74	89.72	75.7	-18.52
	557.05	800.60	59.29	48.4	-22.50

rotor channel space is divided into 84585 body-fitted meshes. Calculations are based on a fixed outlet pressure, obtained from the mass flow rate and the speed of the foreline pump, assuming that foreline conductance can be ignored. Table 6 lists the pumping speeds calculated for this rotor under different outlet conditions. The modeled gas is nitrogen. From the CFD computational results, the simulated inlet pressures can be down to 0.65 Pa with reasonable accuracy, it is belonging to the slip flow regime. Furthermore, when the inlet pressure is further reduced, the continuum assumption inherent to the fluid dynamics is not exactly satisfied owing to the more rarefied gas density, and thus the DSMC simulation approach should be adopted.

In the DSMC simulations, the number of simulated molecules ranges between 600 thousands and 4 million, and the number of cells ranges between 6,000 and 8,000. After performing the DSMC calculations, a three-dimensional steady-state flow field can be observed. Table 6 evaluates five speeds, under inlet pressures of 0.03 Pa, 0.06 Pa, 0.09 Pa, 0.13 Pa, and 0.16 Pa. Notably, the relative errors compared to experimental testing are below 17%.

Figure 8 shows a pumping speed curve fitted by the calculated speeds. This speed curve can then be compared with the experimental testing results to verify the accuracy of the analyses. As Figure 8 shows, the CFD computations predict the pumping speed with an error range from 16.19% to 27.14%. As illustrated in Figure 8, for CFD computations, the relative error to experiment increases with Knudsen number. Computations failed when $\mathrm{Kn} > 0.1$ range. That is, it exceeds the 25% criterion limit. When inlet pressure is below 0.65 Pa, inappropriate use of the CFD method to analyze the rarified gas flow causes a significant increase in the number of computational errors. In this case, the DSMC simulation approach based on molecular kinetic theory must be used to predict the pumping speed in the molecular flow regime. Analyzing a flow in a transitional or viscous regime using the DSMC approach requires far greater computational resources and time than using the CFD approach. Consequently, a compromise between the CFD and DSMC approaches represents the best method of achieving an efficient analysis. When inlet pressure is between 10^{-5} Pa and 1 Pa, the DSMC approach offers the best method of analyzing the problem, and the analytical results reveal an error ranging between 11.89% and 17.36%. For DSMC simulations, decreasing Knudsen number the relative error to experiment is increased. Simulations failed when $\mathrm{Kn} < 0.7$. That is, it exceeds 17% criterion limit. Interestingly, the pumping speed values predicted by DSMC simulation are always smaller than the testing data. One possible explanation for this phenomenon is that the calculated pressures in the analyzing model occur in slightly different locations to the measured pressures. When the Knudsen number in the range of $0.5 < \mathrm{Kn} < 0.1$, neither the CFD computations nor the DSMC simulation are suitable for analyzing the pumping speed of the turbo booster pump.

Finally, from the numerical results displayed in Figure 8, the design methodology combining the CFD and DSMC approaches represents a useful and accurate design tools for prototype design and performance assessment for new varieties of turbo pump.

CONCLUSION

This investigation measured the pumping speed for the spiral-grooved turbo booster pump with well-designed blade geometry and simulates pumping performance using both the CFD and DSMC approaches. The operating pressure range of the pump designed in this study extends from 10^{-5} Pa on the inlet side to several hundred Pascals on the exhaust side. Moreover, this study measured the performance of the pump presented here, and compared it to that of other varieties of turbo pumps. The testing results reveal that this design has a higher foreline capability up to 1000 Pa range than other pumps it was compared with. Consequently, the pump examined here can omit the need for a mechanical booster pump, thus simplifying the pumping system and reducing costs. Since the designed rotor satisfies the pumping characteristics under different pressure ranges, it can be successfully operated at the molecular flow, transitional flow, and viscous flow regimes, respectively. Furthermore, this study also combines CFD and DSMC methodologies for simulating the speeds of the turbo booster pump. The calculation results show that the proposed design procedure is a successful and effective tool in the turbo booster pump's design. Unfortunately, because of the inherent complexity of flow field analysis of the turbo booster vacuum pump and the fundamental limitations of the CFD and DSMC approaches, both of these computational methodologies are inadequate for providing an accurate pumping speed trend in the $0.001 < P_{\mathrm{in}} < 0.01$ Pa range, as shown in Figure 8. Therefore, the experimental approach employed here is the only way of accurately and effectively exploring pump performance in the $0.001 < P_{\mathrm{in}} < 0.01$ Pa range. This investigation aims to demonstrate the effectiveness of the experimental approach for investigating the pumping speed of the turbo booster pump, and the failure of using numerical methods for turbo booster pump analyses in this pressure range. Until now, the literature has neglected this subject. The methods developed here can be applied in the future to design new compound or hybrid turbo pumps.

NOMENCLATURE

A_{in}	inlet area
C	orifice conductance
D	diameter of test dome
D_0	diameter of rotor
d	diameter of the orifice
h_{in}	depth of groove channel at inlet side
h_{out}	depth of groove channel at outlet side
L	length of rotor
L_o	thickness of the orifice plate
M	molecular weight
n_{in}	number density at the inlet side
$N_{\mathrm{in},i}$, $N_{\mathrm{in},o}$	number of the incoming and outgoing molecules

$N'_{\text{in},i}$	inlet influx
P_0, P_1, P_2	ultimate pressure of the test dome, pressure at upper chamber and pressure at lower chamber
Q	throughput
R	universal gas constant
S	volume flow rate (pumping speed)
T	temperature
Δt	time step
U_{in}	free stream velocity outside the inlet port
X, Y, Z	coordinates of inertial frame
x, y, z	coordinates of rotating frame

Greek Symbols

δ	clearance between rotor and casing
ρ	gas density
ϕ_{in}	blade angle at inlet side
ϕ_{out}	blade angle at outlet side
Ω	rotational speed

REFERENCES

Becker, W. 1961. Zur Theorie der Turbomolekularpumpe. *Vakuum Techn.* 10:199.

Bird, G. A. 1994. *Molecular Gas Dynamics and the Direct Simulation of Gas Flows*. Clarendon Press, Oxford.

Chang, Y. W., and Jou, R. Y. 2001. Direct simulation of pumping characteristics in a full 3D model of a single stage TMP. *Applied Surface Science* 169–170:772–776.

Chang, Y. W., Jou, R. Y., Cheng, H. P., and Chen, F. Z. 2001. Pumping performance analyses of a turbo booster pump by direct simulation Monte Carlo method. *Vacuum* 60:291–298.

Cheng, H. P., Jou, R. Y., Chen, F. Z., Chang, Y. W., Iwane, M., and Hanaoka, T. 2000. Three-dimensional flow analysis of spiral-grooved turbo booster pump in slip and continuum flow. *J. Vac. Sci. Technol.* A18(2):543–551.

Duval, P., Raynaud, A., and Saulgeot, C. 1988. Molecular drag pump: Principle, characteristics, and applications. *J. Vac. Sci. Technol.* A6(3):1187.

Gaede, W. 1913. Die Molekularluftpumpe. *Ann. Phys.* 41:337.

Hablanian, M. H. 1994. Comments on the history of high vacuum turbopumps, in *Vacuum Science and Technology—Pioneers of the 20th Century*, AIP Press.

Heldner, M., and Kabelitz, H. P. 1990. Reliability of turbomolecular vacuum pumps: A comparison of rolling element and magnetic bearing systems. *J. Vac. Sci. Technol.* A8(3):2772.

Henning, J. 1988. Thirty years of turbomolecuar pumps: A review and recent developments. *J. Vac. Sci. Technol.* A6(3):1196.

Heo, J. K., and Hwang, Y. K. 2000. DSMC calculations of blade rows of a turbomolecular pump in the molecular and transition flow regions. *Vacuum* 56:133–142.

Holweck, F. 1923. Pompe moléculaire hélicoidale. *C.R. Acad. Sci.* 177:43.

Jou, R. Y., Cheng, H. P., Chang, Y. W., Chen, F. Z., and Iwane, M. 2000. Designs, analyses, and tests of a spiral-grooved turbo booster pump. *J. Vac. Sci. Technol.* A18(3):1016–1024.

Lee, Y. K., and Lee, J. W. 1996. Direct simulation of compression characteristics for a simple drag pump model. *Vacuum* 47(6–8):807–809.

Levi, G. 1992. Combination of turbomolecular pumping stages and molecular drag stages. *J. Vac. Sci. Technol.* A10(4):2619.

Maurice, L. 1974. A new molecular pump. *Jpn. J. Appl. Phys. Suppl.* 2:21.

Nanbu, K., Kubota, H., Igarashi, S., Urano, C., and Enosawa, H. 1991. Performance of spiral grooves on a rotor of turbomolecular pump. *Transactions of Japan Society of Mechanical Engineers B* 57(533):172–177.

Sawada, T., and Nakamura, M. 1990. Spiral grooved visco-vacuum pumps with various groove shapes. *Vacuum* 41(7–9):1833.

Sawada, T., Nakamura, M., and Abumiya, A. 1992. Spiral grooved vacuum pump working in high pressure ranges. *Vacuum* 43(11): 1097.

Sawada, T. 1993. Improvement in the performance of spiral grooved visco-vacuum pumps in coarse vacuum region. *Vacuum* 44(5–7):689.

Schneider, T. N., Katsimichas, S., de Oliveira, C. R. E., and Goddard, A. J. H. 1998. Empirical and numerical calculations in two dimensions for predicting the performance of a single stage turbomolecular pump. *J. Vac. Sci. Technol.* A16(1):175–180.

Siegbahn, M. 1943. A new design for a high vacuum pump. *Ark. Math. Astron. Fys.* 30B:261.